9-Lipoxygenase-Derived Oxylipins Activate Brassinosteroid Signaling to Promote Cell Wall-Based Defense and Limit Pathogen Infection[1]

Ruth Marcos, Yovanny Izquierdo, Tamara Vellosillo, Satish Kulasekaran[2], Tomás Cascón, Mats Hamberg, and Carmen Castresana*

Centro Nacional de Biotecnología-Consejo Superior de Investigaciones Científicas, Cantoblanco, E–28049 Madrid, Spain (R.M., Y.I., T.V., S.K., T.C., C.C.); Division of Physiological Chemistry II, Department of Medical Biochemistry and Biophysics, Karolinska Institutet, S–171 77 Stockholm, Sweden (M.H.); and Energy Biosciences Institute and Plant and Microbial Biology Department, University of California, Berkeley, California 94720 (T.V.)

ORCID IDs: 0000-0001-8056-2828 (T.V.); 0000-0001-6132-8868 (S.K.); 0000-0002-0715-8965 (C.C.).

The oxylipins, a large family of oxygenated lipid derivatives, regulate plant development and immunity. Two members of the 9-lipoxygenase (9-LOX) oxylipin pathway, 9-hydroxyoctadecatrienoic acid and 9-ketooctadecatrienoic acid, control root development and plant defense. Studies in Arabidopsis (*Arabidopsis thaliana*) using a series of 9-hydroxyoctadecatrienoic acid- and 9-ketooctadecatrienoic acid-insensitive *nonresponding to oxylipins* (*noxy*) mutants showed the importance of the cell wall as a 9-LOX-induced defense component and the participation of NOXY proteins in signaling cell wall damage. Here, we examined 9-LOX signaling using the mutants *lox1lox5*, which lacks 9-LOX activity, and *noxy2-2*, which shows oxylipin insensitivity and mitochondrial dysfunction. Mutants in brassinosteroids (BRs), a class of plant hormones necessary for normal plant growth and the control of cell wall integrity, were also analyzed. Several lines of evidence indicated that 9-LOX-derived oxylipins induce BR synthesis and signaling to activate cell wall-based responses such as callose deposition and that constitutive activation of BR signaling in *bri1-EMS-suppressor 1-D* (*bes1-D*) plants enhances this response. We found that constitutive BR signaling in *bes1-D* and *brassinolide-resistant 1-1D* (*bzr1-1D*) mutants conferred resistance to *Pseudomonas syringae*. *bes1-D* and *bzr1-1D* showed increased resistance to *Golovinomyces cichoracearum*, an obligate biotrophic fungus that penetrates the cell wall for successful infection, whereas susceptibility was enhanced in *lox1lox5* and *noxy2-2*. Our results indicate a sequential action of 9-LOX and BR signaling in activating cell wall-based defense, and this response prevents pathogen infection. These results show interaction between the 9-LOX and BR pathways and help to clarify their role in modulating plant defense.

In plants, pathogen attack activates a complex defense response that limits their ingress and tissue invasion. These responses are activated by the perception of pathogen molecules such as microbial-associated molecular patterns and effector proteins as well as by the recognition of plant compounds produced during infection (Boller and Felix, 2009). Data indicate that, among the latter, cell damage-associated molecular pattern molecules are produced after biotic stress as a mechanism to monitor and maintain functional cell wall integrity (Ferrari et al., 2013). Plants trigger ubiquitous responses, such as alkalinization, transient ion changes, and reactive oxygen species (ROS) production, following the activation of receptors that regulate growth and immunity (Dangl et al., 2013; Wrzaczek et al., 2013; Macho and Zipfel, 2014; Wolf and Höfte, 2014). Surveillance and control mechanisms confer specificity on these responses to activate distinct hormone pathways, although different processes can share signaling events.

Oxylipins are among the signaling molecules involved in regulating plant development and immunity (López et al., 2008; Andreou et al., 2009; Kachroo and Kachroo, 2009). The biosynthesis of plant oxylipins is initiated by the action of 9- and 13-lipoxygenases, α-dioxygenases (α-DOX), or monooxygenases, all of which predominantly catalyze the oxygenation of linolenic acid (18:3) and linoleic acid (18:2) into reactive hydroperoxides, followed by secondary modification catalyzed mainly by cytochrome P450 enzymes or peroxygenases (Blée, 2002; Hamberg et al., 2002, 2003; Andreou et al., 2009; Zoeller et al., 2012). Oxylipins can also be produced nonenzymatically from polyunsaturated fatty acids in the

[1] This work was supported by the Spanish Ministry of Economy and Competitiveness (grant no. BIO2012–33954) and the La Caixa Foundation International Fellowship Program (Ph.D. fellowships to S.K. and Y.I.).

[2] Present address: Biosciences, Molecular Plant Pathology, College of Life and Environmental Sciences, University of Exeter, Exeter EX4 4QD, UK.

* Address correspondence to ccastresana@cnb.csic.es.

The author responsible for distribution of materials integral to the findings presented in this article in accordance with the policy described in the Instructions for Authors (www.plantphysiol.org) is: Carmen Castresana (ccastresana@cnb.csic.es).

R.M., Y.I., and C.C. designed the research; R.M., Y.I., S.K., T.V., and T.C. performed the research; R.M., Y.I., S.K., T.V., T.C., and C.C. analyzed the data; M.H. contributed the reagents/analytic tools; C.C. wrote the article.

www.plantphysiol.org/cgi/doi/10.1104/pp.15.00992

presence of singlet oxygen or by free radical-mediated oxygenation (Durand et al., 2009).

The jasmonate pathway of the oxylipin metabolome is initiated by 13-lipoxygenase (13-LOX) to form (+)-7-iso-jasmonic acid and its Ile conjugate; these compounds stimulate transcription programs that control plant resistance to necrotrophic pathogens, wounding, and insect attack (Browse, 2009; Fonseca et al., 2009; Wu and Baldwin, 2010; Wasternack and Hause, 2013). The jasmonate pathway also regulates physiological processes such as fertility, senescence, and mechanotransduction (Santino et al., 2013). A number of other studies show that oxylipins produced by the α-DOX pathway participate in plant senescence and development (Obregón et al., 2001; Bannenberg et al., 2009) and that α-DOX enzymes localize in lipid bodies formed in senescent leaves and in leaves responding to pathogen infection (Shimada et al., 2014).

The importance of the 9-LOX pathway in plant responses to pathogen and pest attack was recently defined (Hwang and Hwang, 2010; López et al., 2011; Nalam et al., 2012). Genetic studies in Arabidopsis (*Arabidopsis thaliana*) showed a 9-LOX function in activating local defense and stomata closure against virulent *Pseudomonas* spp. (Hwang and Hwang, 2010; López et al., 2011; Montillet et al., 2013) as well as 9-LOX and α-DOX pathway cooperation in triggering systemic resistance (Vicente et al., 2012). There is also evidence of a role in activating systemic defense for C9 oxylipins formed by nonenzymatic free radical reactions (Jung et al., 2009; Wang et al., 2014; Wittek et al., 2014).

Analyses of the signaling processes that mediate the action of 9-LOX derivatives indicated their role as regulators of root development and defense responses via a (+)-7-iso-jasmonic acid-independent pathway that might be involved in cell wall modification (Vellosillo et al., 2007). Studies using *nonresponding to oxylipins* (*noxy*) mutants with an impaired response to the 9-LOX product 9-hydroxyoctadecatrienoic acid (9-HOT) showed that the 9-LOX signaling defect frequently coincides with enhanced insensitivity to isoxaben (Vellosillo et al., 2013), an herbicide that inhibits cellulose synthesis and triggers cell wall repair responses (Manfield et al., 2004; Hamann et al., 2009). These findings showed the importance of the cell wall as a component of 9-LOX-induced defense and the participation of NOXY proteins in signaling cell wall responses.

Here, we characterized the signaling processes that mediate the action of 9-LOX-derived oxylipins as inducers of cell wall-based defense. Using *lox1lox5* mutants that lack 9-LOX activity and the 9-LOX signaling mutant *noxy2-2*, we found that 9-LOX-derived oxylipins require brassinosteroid (BR) synthesis as well as active BR signaling to induce cell wall-based defenses and limit pathogen infection.

RESULTS

The 9-LOX and BR Pathways Share Signaling Components

Our previous studies of 9-LOX derivative action indicated their role as inducers of cell wall modifications and root waving (Vellosillo et al., 2007). Characterization of *noxy* mutants showed that the 9-LOX pathway participates in signaling cell wall damage (Vellosillo et al., 2013). These 9-LOX pathway characteristics parallel the functions reported for BRs, whose signaling is triggered as part of a compensatory mechanism to maintain cell wall integrity; application of 24-epibrassinolide (BL; an active BR) to Arabidopsis seedlings induces root waving that resembles the oxylipin phenotype (Lanza et al., 2012; Wolf et al., 2012; Wolf and Höfte, 2014). These observations suggested that the 9-LOX and BR pathways share signaling components.

To test this possibility, we compared the response to 9-LOX and BR products of wild-type, *lox1lox5* (which lacks 9-LOX activity; López et al., 2011), *deetiolated2-1* (*det2-1*; whose BR biosynthesis is impaired; Fujioka et al., 1997), and *bri1-1* (which does not sense BR; Friedrichsen et al., 2000) plants. Compared with the phenotype of seedlings grown on Murashige and Skoog (MS) medium (Fig. 1A), treatment with 9-HOT, 9-ketooctadecatrienoic acid (9-KOT), or BL induced root waving in wild-type and *lox1lox5* plants, whereas this response was strongly suppressed in *bri1-1* mutants (Fig. 1, B–D). BL induced root waving and complemented the *det2-1* phenotypic alteration (Fig. 1D), although the mutant did not respond to 9-HOT or 9-KOT (Fig. 1, B and C; Table I). These findings suggested that the BR pathway participates in 9-LOX signaling and that 9-HOT and 9-KOT act upstream of BR biosynthesis and signaling. These results were supported by data showing that the BR synthesis inhibitor BZ impaired the root-waving activities of 9-HOT and 9-KOT in wild-type plants (Fig. 1, B and C) but did not interfere with root waving in response to BL (Fig. 1D).

In addition, we examined the expression of the *ABC transporter* (*ABC*) and *FAD-binding oxidoreductase* (*FOX*) genes, which are up-regulated by 9-HOT and 9-KOT (López et al., 2011; Vicente et al., 2012), and found that the expression induced in response to 9-KOT was greatly reduced in *det2-1* compared with wild-type plants (Fig. 1E), which supports BR participation in 9-LOX signaling.

The 9-LOX Oxylipins Activate the BR Pathway

Having determined that the BR pathway participates in 9-LOX signaling, we evaluated the effect of 9-HOT and 9-KOT on BR biosynthesis and signaling. We examined BR synthesis in *DWARFISM4* (*DWF4*):*GUS* transgenic seedlings, in which the promoter of the *DWF4* gene involved in BR biosynthesis directs the expression of the GUS reporter (Chung et al., 2011). GUS staining was observed in root primordia of control *DWF4*:*GUS* seedlings and was increased in roots and emerging leaves after 9-HOT or 9-KOT treatment (Fig. 2A). We used the transgenic line BKI1:YELLOW FLUORESCENT PROTEIN (YFP), which expresses the early BR signaling marker BRASSINOSTEROID KINASE INHIBITOR1 (BKI1; Wang and Chory, 2006), to test whether 9-LOX compounds trigger BR signaling. BKI1

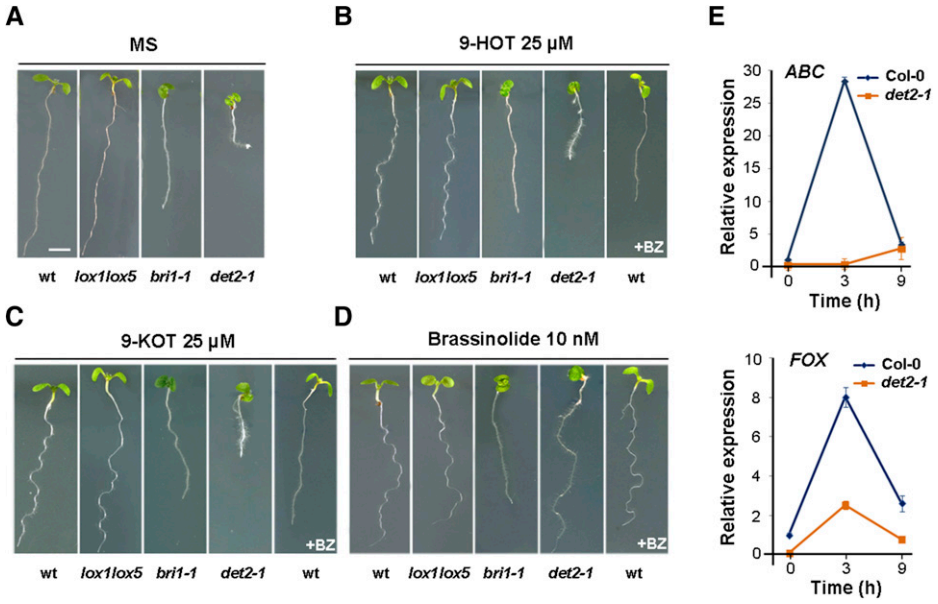

Figure 1. Response of wild-type (wt), *lox1lox5*, *bri1-1*, and *det2-1* plants to 9-HOT, 9-KOT, and BL. A, Phenotypes of plants grown on MS medium (3 d) and transferred to fresh MS control medium (4 d). B, Phenotypes of plants grown on MS medium (3 d) and transferred to MS medium containing 9-HOT (25 μM; 4 d). At right, the phenotype of wild-type plants transferred to MS medium containing 9-HOT (25 μM) and brassinazole (BZ; 1 μM) is shown. C, Phenotypes of plants grown on MS medium (3 d) and transferred to MS medium containing 9-KOT (25 μM; 4 d). At right, the phenotype of wild-type plants transferred to MS medium containing 9-KOT (25 μM) and BZ (1 μM) is shown. D, Phenotypes of plants grown on MS medium (3 d) and transferred to MS medium containing BL (10 nM; 4 d). At right, the phenotype of wild-type plants transferred to MS medium containing BL (10 nM) and BZ (1 μM) is shown. Bar in A = 250 μm. E, *ABC* and *FOX* expression in wild-type Columbia-0 (Col-0) and *det2-1* plants determined by quantitative reverse transcription (RT)-PCR analysis in RNA samples extracted at different times from 25 μM 9-KOT-treated seedlings. The gene *At1g43170* encoding Ribosomal protein L3A was used to normalize transcript levels in each sample. Data shown are mean ± SE of three independent experiments.

is an inhibitory protein that dissociates from the BR receptor after BR activation and relocalizes from the plasma membrane to the cytosol. We tested whether 9-HOT and 9-KOT treatment led to BKI1:YFP displacement and, thus, to the activation of BR signaling. YFP fluorescence in roots of untreated seedlings was located mainly at the cell membrane and, to a lesser extent, in the cytoplasm (Fig. 2B). At 5 h after BL treatment, most YFP fluorescence relocalized from the membrane to the cytoplasm. BKI1:YFP redistributed similarly from the membrane to the cytosol at 5 h after 9-HOT and 9-KOT application, confirming the activation of BR signaling (Fig. 2B).

A third process used to evaluate BR signaling involvement in the response to 9-LOX oxylipins was the activation of BRASSINOLIDE-RESISTANT1 (BZR1) and BRI1-ETHYL METHANESULFONATE-SUPPRESSOR1 (BZR2/BES1), two key transcription factors that govern BR signaling whose activity is negatively regulated by phosphorylation (Wang et al., 2002; Yin et al., 2002). In transgenic plants expressing chimeric BZR1-CYAN FLUORESCENT PROTEIN (CFP) or BZR2/BES1-GFP (Wang et al., 2002; Yin et al., 2002), we tested BZR1 and BZR2/BES1 phosphorylation levels in 7-d-old transgenic seedlings in liquid MS medium, untreated or treated with BL, 9-HOT, or 9-KOT (Fig. 2C; Supplemental Fig. S1). BL treatment led to progressive dephosphorylation of BZR1 and BRZ2/BES1 in seedlings starting at 3 h after application. Dephosphorylation of BZR1 and BZR2/BES1 was earlier and more pronounced when BL was combined with 9-HOT and 9-KOT, whereas there were no changes in BZR1 or BZR2/BES phosphorylation after the application of 9-HOT or 9-KOT alone (Fig. 2C; Supplemental Fig. S1).

9-LOX Oxylipin-Mediated Cell Wall Modification Requires BR Synthesis and Signaling

We previously showed the action of 9-LOX derivatives as inducers of cell wall changes, including the formation of callose deposits (Vellosillo et al., 2007). As 9-HOT and 9-KOT activate BR signaling, we tested whether the callose formation activity of these oxylipins is mediated by the activation of BR signaling. We examined callose production in response to 9-HOT in *bri1-1* and *det2-1* mutants, which show impaired BR perception and biosynthesis, respectively. In these analyses, we used *bes1-D* and *bzr1-1D* mutants with constitutive activation of BR signaling (Wang et al., 2002; Yin et al., 2002) as well as the 9-HOT-insensitive *noxy2-2* mutant (Vellosillo et al., 2013). As seen in Figure 3A, no callose deposits were detected in roots of wild-type plants after Aniline Blue staining. Wild-type seedling growth in 9-HOT-containing medium induced

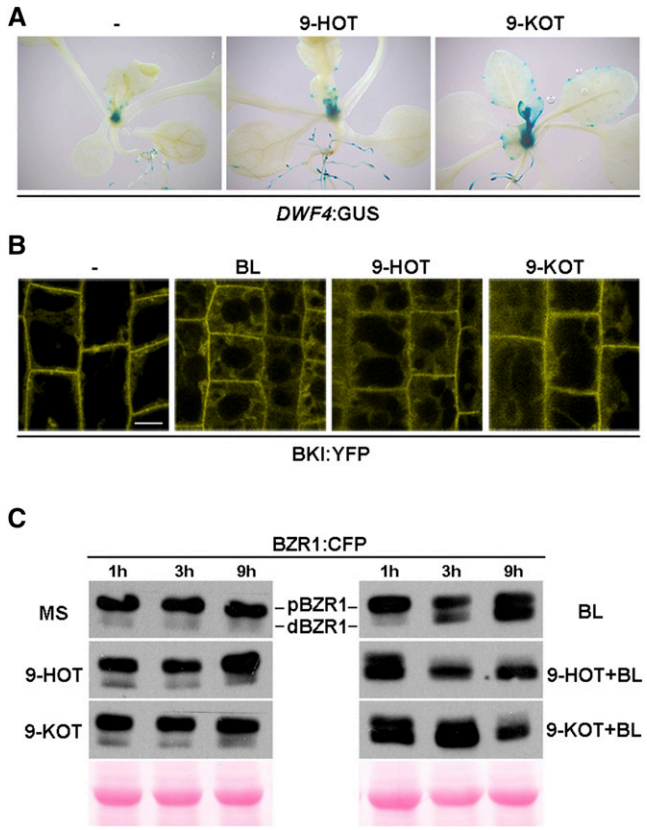

Figure 2. Activation of BR synthesis and signaling by 9-HOT and 9-KOT. A, Histological examination of GUS activity in 12-d-old seedlings of a *DWF4:GUS* transgenic line grown in MS medium and transferred (3 h) to MS medium with 9-HOT (25 μM) or 9-KOT (25 μM). B, Confocal images of 35S:BKI:YFP roots grown on MS medium (6 d) and treated (5 h) with BL (10 nM), 9-HOT (25 μM), or 9-KOT (25 μM). Bar = 10 μm. C, Analyses of BZR1-CFP protein phosphorylation in 6-d-old seedlings grown in the dark on MS medium and transferred to MS medium with BL (50 nM), 9-HOT (25 μM), or 9-KOT (25 μM) alone or with BL combined with 9-HOT (25 μM) or 9-KOT (25 μM). Protein was extracted and examined at the indicated times. An anti-GFP antibody was used for immunoblots. Ponceau Red staining (0.1%) was used as a control for protein loading.

root waving, with the formation of numerous callose deposits, whereas the two BR-deficient mutants, *bri1-1* and *det2-1*, did not show these responses (Fig. 3B; Table I). Treatment with BL combined with 9-HOT restored root waving and callose accumulation in *det2-1* but not in *bri1-1* plants, which indicated that callose production in response to 9-HOT requires BR synthesis and signaling; we also observed that the BR synthesis inhibitor BZ impaired callose induction by 9-HOT in wild-type plants (Fig. 3B). Treatment of wild-type seedlings with BL (or BZ) alone did not activate the formation of callose deposits; BRs are thus not sufficient to trigger this cell wall modification (Fig. 3A). No callose deposits were found in untreated roots of *bes1-D* and *bzr1-1D* plants. Compared with wild-type plants, *bes1-D* mutants showed enhanced accumulation of callose after 9-HOT application, whereas we detected no major differences from wild-type plants in *bzr1-1D* mutants (Fig. 3C). The 9-HOT-insensitive *noxy2-2* mutant did not form callose deposits in response to 9-HOT, a defect that was not complemented by simultaneous application of BL (Fig. 3B). The results of these analyses indicated that callose production in response to 9-HOT requires active 9-LOX and BR signaling pathways and that the constitutive activation of BR signaling in *bes1-D* mutants facilitates 9-HOT action as a cell wall modifier.

The *noxy2-2* Mutation Disturbs 9-LOX But Not BR Signaling

Given the role of BR in signaling the activities of 9-LOX-derived oxylipins, we tested whether the 9-HOT-insensitive *noxy2-2* mutant showed additional BR signaling defects. To examine this possibility, we compared the response to 9-KOT and BL of *noxy2-2* and wild-type plants as well as the *lox1lox5* mutant, which is defective in 9-LOX-derived oxylipin synthesis. As reported previously (Vellosillo et al., 2013), the *noxy2-2* seedling phenotype revealed shorter roots than those of wild-type plants. As anticipated, *noxy2-2* did not induce root waving in response to 9-KOT (Fig. 4A). Analysis of *ABC* and *FOX* gene expression showed that the transcript level induced in response to 9-KOT was reduced in *noxy2-2* compared with wild-type plants (Fig. 4B). In contrast to oxylipins, *noxy2-2* responded to BL by inducing root waving (Fig. 4A). We also found that the levels of the BR-inducible gene *EXPANSIN8* (*EXP8*; At2g40610) after BL treatment were similar in *noxy2-2* and wild-type plants (Fig. 4C). The *lox1lox5* mutant, which responds to 9-KOT and BL by inducing root waving (Fig. 1, B–D), responded to these treatments by inducing transcript levels similar to those of wild-type plants (*ABC* and *FOX* for 9-KOT and *EXP8* for BL; Fig. 4, B and C).

Hypocotyl elongation is frequently used to evaluate BR production and signaling (Weigel and Glazebrook, 2008); we evaluated this response to further analyze *noxy2-2*. *noxy2-2*, *lox1lox5*, and wild-type plants were germinated in different light conditions (long day and high light intensity versus short day and low light intensity), and hypocotyl length was measured in seedlings 7 d postgermination; *det2-1*, *bes1-D*, and *bzr1-1D* mutants in the BR pathway were also included in these analyses (Fig. 4D). *noxy2-2* plant hypocotyls elongated at a rate similar to that of wild-type and *lox1lox5* plants (Fig. 4, E and F), suggesting that BR production and signaling are not impaired in *noxy2-2* and *lox1lox5* mutants. No significant differences in hypocotyl length or elongation were detected between *bzr1-1D* and wild-type plants, whereas the hypocotyls of *bes1-D* mutants elongated at a higher rate, which might be indicative of a higher activation of BR signaling (Fig. 4, E and F). Consistent with the BR biosynthesis defect, a minor hypocotyl elongation was detected in *det2-1* mutants (Fig. 4, E and F).

The results of these studies indicated that the *noxy2-2* mutation acts upstream of BR in the 9-LOX signaling

Table I. *Description of plants and responses to the treatments examined*
Dashes indicate not observed.

Genotype	Description	Oxylipin-Induced Waving	BL-Induced Waving	Oxylipin-Induced Callose	*Pst* DC3000-Induced Callose	*Pst* DC3000 Susceptibility	*G. cichoracearum* Susceptibility
Columbia-0	Wild type	+	+	+	+	Susceptible	Susceptible
det2-1	Deficient in BR synthesis	−	+	−			
bri1-1	Impaired in BR signaling	−	−	−			
bes1-D	Constitutively activated BR signaling	+	+	+	Above Columbia-0	Enhanced resistance	Enhanced resistance
bzr1-1D	Constitutively activated BR signaling	+	+	+	+	Enhanced resistance	Enhanced resistance
lox1lox5	Deficient in 9-LOX products	+	+	+	+	Enhanced susceptibility	Enhanced susceptibility
noxy2-2	Impaired in 9-LOX signaling	−	+	−	Below Columbia-0	Enhanced susceptibility	Enhanced susceptibility

pathway and that this mutation probably affects the signaling processes that mediate 9-LOX derivative action as activators of BR signaling.

Activation of BR Signaling Enhances Cell Wall-Based Defense

The accumulation of callose deposits helps to reinforce the cell wall and prevent infection and is a common marker of plant defense against pathogen attack (Vorwerk et al., 2004; Luna et al., 2011). 9-LOX derivatives induce the formation of callose deposits; therefore, it was of interest to test whether the 9-LOX and BR signaling pathways participate in inducing this cell wall modification in bacterially infected plant leaves. The pronounced leaf development defect in *bri1-1* and *det2-1* mutants impedes their use for bacterial inoculation; for these studies, we used *bes1-D* and *bzr1-1D* mutants, both with constitutive activation of BR signaling (Wang et al., 2002; Yin et al., 2002), as well as *lox1lox5* and the 9-LOX signaling mutant *noxy2-2*. The virulent *Pseudomonas syringae* pv *tomato* (*Pst*) DC3000 was used for inoculation. Whereas no callose deposits formed in control leaves infiltrated with $MgCl_2$, *Pst* DC3000 (10^6 colony-forming units [cfu] mL^{-1}) induced the formation of callose deposits in wild-type plants (Fig. 5). There was a significant increase in callose deposits in *bes1-D* plants, whose number and size were augmented approximately 2.3- and 1.8-fold, respectively, above wild-type plant levels (Fig. 5, B–D). This response contrasted with the results in *noxy2-2* mutants, in which the number and size of callose deposits were reduced significantly (approximately 2.7- and 2-fold, respectively) relative to wild-type plants (Fig. 5, B–D). Analyses of *lox1lox5* and *bzr1-1D* mutants showed no variations in callose deposit production compared with wild-type plants (Fig. 5, B–D; Table I).

Activation of BR Signaling Enhances Plant Resistance to Biotrophic Pathogens and Interferes with Pathogen Penetration

Our results indicated that the formation of callose deposits in response to *Pst* DC3000 varies significantly among the mutants examined. Consistent with a positive role of callose in restricting pathogen infection, the enhanced susceptibility of *noxy2-2* to *Pst* DC3000 (Vellosillo et al., 2013) was accompanied by decreased production of this cell wall polysaccharide. Therefore, we predicted that greater callose accumulation would increase the defense potential of *bes1-D* plants to *Pst* DC3000 infection and examined the phenotype of *bes1-D* for enhanced

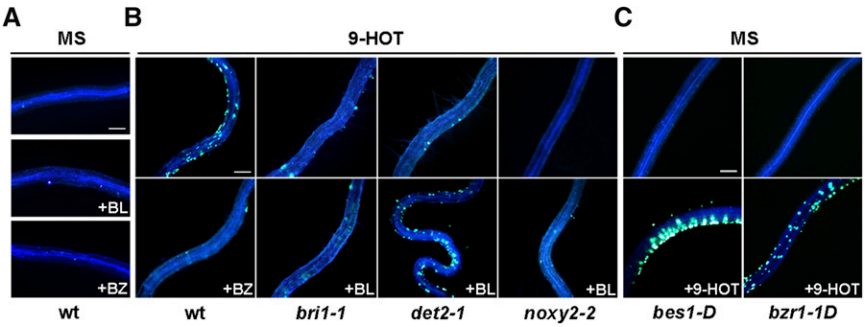

Figure 3. Formation of callose deposits in roots of wild-type (wt) and mutant plants after 9-HOT treatment. A, Aniline Blue staining of wild-type plants grown on MS alone or treated with BZ (1 μM) or BL (10 nM). B, Fluorescence of callose deposits by Aniline Blue staining in 9-HOT-treated roots (25 μM) of wild-type, *bri1-1*, *det2-1*, and *noxy2-2* plants. The bottom row shows callose deposition in roots treated in addition with BZ (1 μM) or BL (10 nM). C, *bes1-D* and *brz1-1D* plants grown on MS or treated with 9-HOT. Bars = 100 μm.

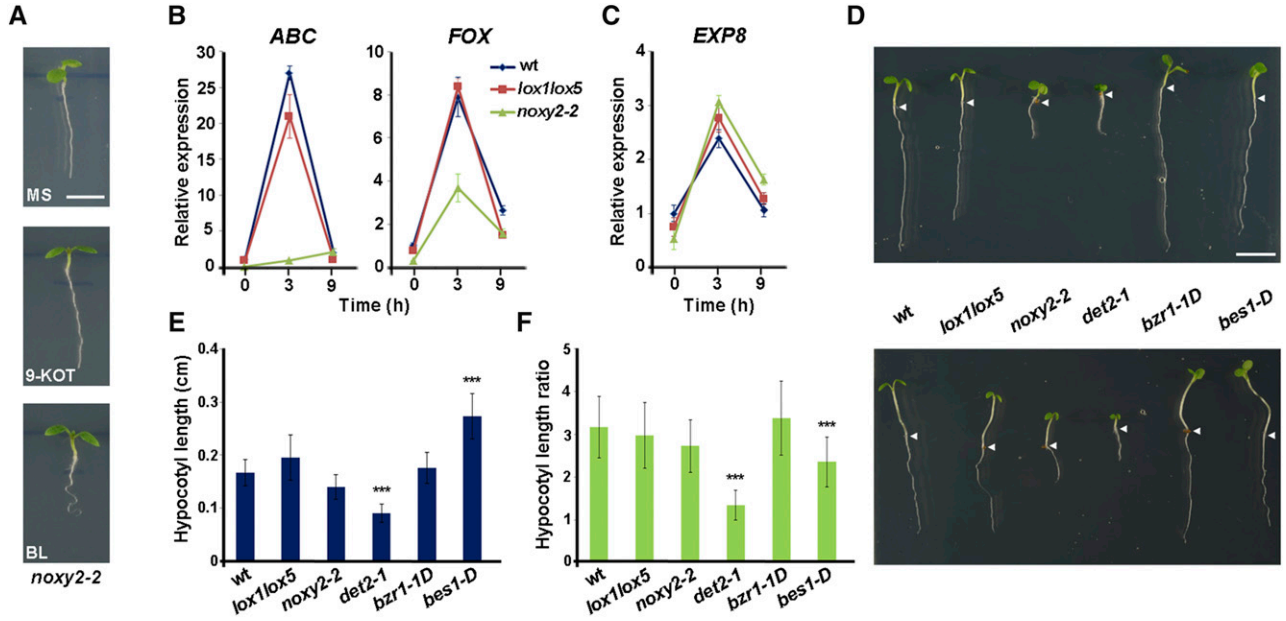

Figure 4. *noxy2-2* response to BR. A, Phenotypes of *noxy2-2* plants grown on MS medium (3 d) and transferred to fresh MS medium (4 d) alone or containing 9-HOT (25 μM) or BL (10 nM). Bar = 250 μm. B, *ABC* and *FOX* expression in wild-type (wt), *lox1lox5*, and *noxy2-2* plants was determined by quantitative RT-PCR analysis in RNA samples extracted at different times from 25 μM 9-KOT-treated seedlings. C, *EXP8* expression in wild-type, *lox1lox5*, and *noxy2-2* plants determined by quantitative RT-PCR analysis in RNA samples extracted at different times from BL-treated seedlings. The gene *At1g43170* encoding RPL3A was used to normalize transcript levels in each sample. Data shown are means ± SE of three independent experiments. D, Phenotypes of wild-type, *lox1lox5*, *noxy2-2*, *det2-1*, *bzr1-1D*, and *bes1-D* seedlings grown on MS medium (6 d) in long-day and high light intensity (top) or short-day or low light intensity (bottom) conditions (see "Materials and Methods"). Arrowheads indicate root/shoot junctions. Bar = 500 μm. E, Hypocotyl lengths of wild-type, *lox1lox5*, *noxy2-2*, *det2-1*, *bzr1-1D*, and *bes1-D* seedlings grown on MS medium (6 d) in long-day and high light intensity conditions. Data shown are means ± SE of three independent experiments (n = 30). Asterisks above the bars indicate statistically significant differences between the wild type and mutants examined (one-way ANOVA and Games-Howell test; $P < 0.001$). F, Ratio of hypocotyl lengths of wild-type, *lox1lox5*, *noxy2-2*, *det2-1*, *bzr1-1D*, and *bes1-D* seedlings grown (6 d on MS medium) in long-day and high light intensity or short-day and low light intensity conditions (see "Materials and Methods"). Data shown are means ± SE of three independent experiments (n = 30). Asterisks above the bars indicate statistically significantly differences between the wild type and mutants examined (one-way ANOVA and Games-Howell test; $P < 0.001$).

resistance to *Pst* DC3000 as well as that of the *bzr1-1D* mutant. Three days after bacterial inoculation, *Pst* DC3000 growth in *bes1-D* leaves was reduced by 10-fold compared with wild-type plants (Fig. 6A), indicating that the enhanced callose production in *bes1-D* correlates with reduced pathogen infection. In *bzr1-1D*, although there was no variation in callose deposit formation, bacterial growth was reduced approximately 2-fold compared with wild-type plants (Fig. 6A; Table I). Accompanying the reduction in bacterial growth, both *bes1-D* and *bzr1-1D* showed milder disease symptoms than those in wild-type plants (Fig. 6, B and C). Thus, strong disease symptoms (type III) were reduced from approximately 70% in wild-type plants to 18% and 30% in *bes1-D* and *bzr1-1*, respectively (Fig. 6, B and C). These results indicated that the constitutive activation of BR signaling in *bes1-D* and *bzr1-1D* promotes plant defense and suggest that, in addition to callose, other defensive mechanisms mediate plant defense in BR constitutive mutants.

As the cell wall is a defense barrier that limits pathogen ingress, we further studied the cell wall-modifying activity of the 9-LOX and BR pathways using *Golovinomyces cichoracearum*, an obligate biotrophic fungus that penetrates the epidermal cell wall to feed from living cells and grow epiphytically, producing white pustules (Micali et al., 2008). Spores were sprayed onto wild-type plants and 9-LOX and BR mutants; to follow disease progression, we visualized hypha growth on the leaf surface and Coomassie Brilliant Blue stained infected leaves. Epiphytic growth was abundant in wild-type plants at 8 d postinoculation. Fungal growth was increased in *lox1lox5* and *noxy2-2* compared with wild-type plants, whereas leaves of *bes1-D* and *bzr1-1D* mutants showed less hyphae production (Fig. 7A; Table I). Coomassie Blue staining of infected leaves showed large amounts of hyphae in wild-type plants. *lox1lox5* and *noxy2-2* mutants showed a clear increase in the amount of conidia, whereas hyphae accumulation was markedly reduced in *bes1-D* and *bzr1-1D* mutants, to levels below those of wild-type plants (Fig. 7B). As fungal growth on the leaf surface is sustained by feeding structures formed after cell wall penetration, the great reduction in fungi in *bes1-D* and *bzr1-1D* plants is consistent with reduced penetration and probably with cell wall reinforcement.

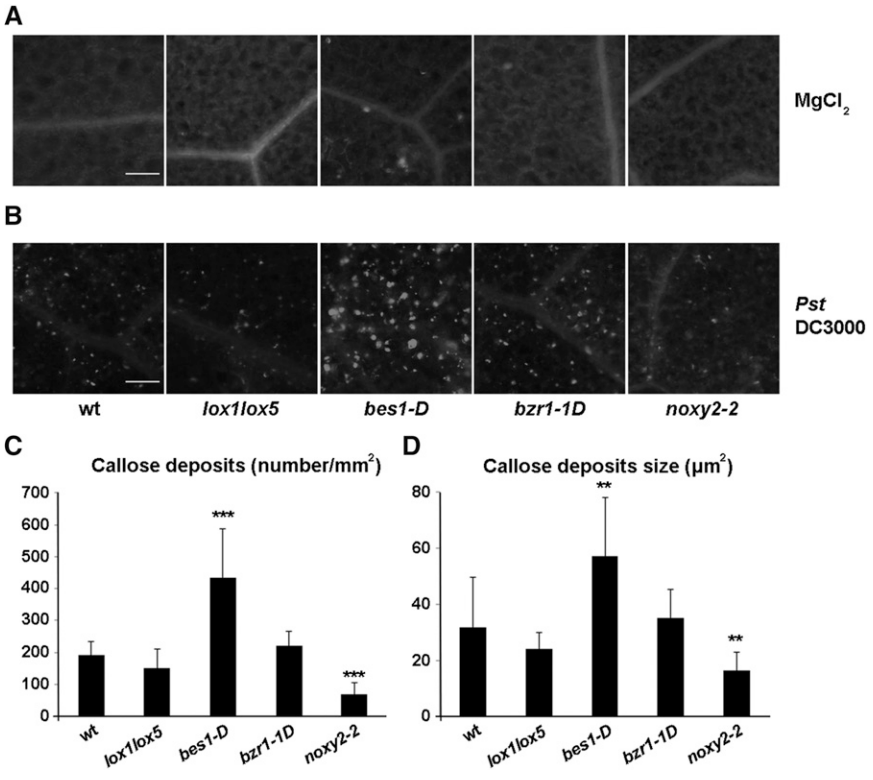

Figure 5. Characterization of callose formation in leaves after *Pst* DC3000 inoculation. A, Fluorescence of callose deposits in leaves of wild-type (wt), *lox1lox5*, *bes1-D*, *bzr1-1D*, and *noxy2-2* plants infiltrated with $MgCl_2$ (10 mM). B, Fluorescence of callose deposits in leaves of plants as above infiltrated with *Pst* DC3000 (10^6 cfu mL^{-1}). Bars = 100 μm. C, Number of callose deposits formed after bacterial inoculation. D, Size of callose deposits formed after bacterial infiltration. Asterisks indicate significant differences between wild-type seedlings and mutants: ***, $P < 0.001$; and **, $0.001 < P < 0.01$ (Student's *t* test). All leaves were stained with Aniline Blue 24 h after treatment.

Conversely, enhanced fungal growth in 9-LOX mutants could be the result of a weakened cell wall. Further analyses are needed to test these possibilities; nonetheless, our results are consistent with the participation of 9-LOX and BR signaling in promoting cell wall changes, thus helping to reinforce this cellular barrier and prevent pathogen infection.

DISCUSSION

The 9-LOX derivatives 9-HOT and 9-KOT activate cell wall-based defense responses, and the 9-LOX oxylipin pathway participates in signaling cell wall damage (López et al., 2011; Vicente et al., 2012; Vellosillo et al., 2013). The latter activity, as well as the oxylipin-induced root-waving response, closely resembles the characteristics of BR as activators of cell wall repair and root waving (Wolf et al., 2012; Wolf and Höfte, 2014). These coincidences, which are indicative of shared signaling events between the 9-LOX and BR pathways, were studied here using 9-LOX and BR mutants impaired in the biosynthesis and signaling processes that govern the actions of these two types of signal compounds.

Consistent with the activities common to the 9-LOX and BR signaling pathways, our results with *bri1-1* and *det2-1* mutants (defective in BR signaling and synthesis, respectively) showed that, for their activity, 9-HOT and 9-KOT require BR synthesis and signaling and that these oxylipins act upstream of BR. Data showing mediation of the three oxylipin-triggered activities via BR signaling (induction of root waving, up-regulation of gene expression, and formation of callose deposits) indicate a BR pathway requirement for 9-LOX signaling. In accordance, comparison of the transcription profile of leaves that responded to 9-KOT (Vicente et al., 2012) with a compendium of BR-responsive genes from various microarray studies (Sun et al., 2010) showed that 9-KOT up-regulated transcripts are significantly enriched in BR-induced (24%) and BR-repressed (12%) genes as well as in direct targets of BZR1 (34%), a key transcription factor that controls BR signaling (Supplemental Fig. S2).

Additional studies with transgenic marker lines supported 9-LOX oxylipins as inducers of BR synthesis and signaling (Fig. 2). The 9-KOT and 9-HOT induction of GUS activity in young leaves and roots of *DWF4*:*GUS* lines is consistent with increased BR biosynthesis in response to these oxylipins. Moreover, BKI1:YFP displacement from the cell membrane to cytoplasm after BL, 9-HOT, or 9-KOT treatment indicates the activation of BR signaling. The synergistic activity of 9-LOX-derived oxylipins and BR in facilitating BZR1 and BZR2/BES1 dephosphorylation supports a function for oxylipins as BR signaling activators. We observed the induction of GUS activity in *DWF4*:*GUS* seedlings and BKI1:YFP mobilization in young growing tissues (Fig. 2), in which BR might regulate plant growth (Zhu et al., 2013). This local BR pathway induction might explain our results for BZR1 and BZR2/BES1 activation, which showed no change in BZR1 and BZR2/BES1 phosphorylation when total protein extracts from 9-HOT- or 9-KOT-treated seedlings were examined, whereas simultaneous

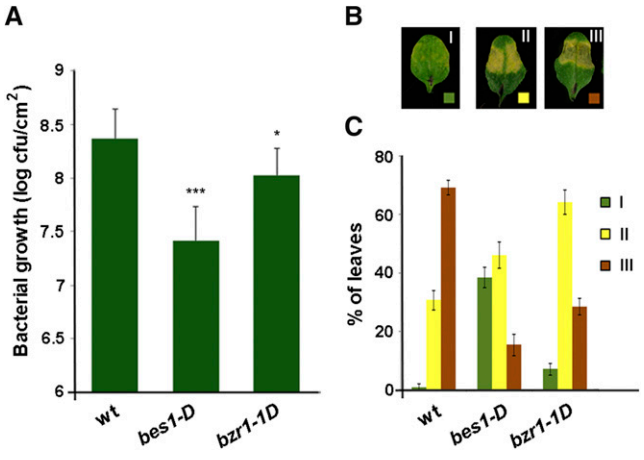

Figure 6. Responses of wild type (wt), *bes1-D*, and *brz1-1D* plants to bacterial infiltration. A, Bacterial growth at 72 h after infiltration of a *Pst* DC3000 suspension (10^5 cfu mL^{-1}). Values shown are means ± SE ($n = 3$ independent experiments). Asterisks indicate significant differences between the wild type and *bes1-D* and *brz1-1D* mutants: ***, $P < 0.001$; and *, $0.01 < P < 0.01$ (Student's *t* test). B, Bacterial symptoms developed at 3 d after inoculation with *Pst* DC3000 (10^6 cfu mL^{-1}) scored on a three-point scale, designated I, II, and III, according to intensity (described in "Materials and Methods"). The photographs shown are representative examples of more abundant symptoms in *bes1-D* (I), *bzr1-1* (II), and wild-type plants (III). C, Percentages of leaves showing each of the symptoms scored in wild-type, *bes1-D*, and *brz1-1D* plants as indicated in B.

application of oxylipin and BL enhanced BZR1 dephosphorylation compared with that of seedlings treated with BL alone. Exogenous application of 9-HOT or 9-KOT combined with BL might facilitate the oxylipin activation of the BR pathway in a larger number of cells and tissues, thus enhancing the visualization of protein dephosphorylation. In this manner, both types of compounds would act in coordination, and the intensity of activity would be determined by the amount of compounds produced in each specific tissue and physiological condition. This idea is supported by our finding that 9-HOT caused greater callose deposition in *bes1-D* mutants with constitutively activated BR signaling than in wild-type plants (Fig. 3C).

The increased callose accumulation in bacterially infected *bes1-D* mutants corroborates 9-LOX and BR signaling cooperativity in mediating cell wall changes. In this response, constitutive BR signaling facilitates the cell wall-modifying activity of oxylipins, which are produced as part of the plant defense response to counteract *Pseudomonas* spp. infection (Vicente et al., 2012; Zoeller et al., 2012). In a previous study, we found that, in addition to 9-LOX, other oxylipins produced in the 13-LOX and α-DOX pathways activate root waving and the formation of callose deposits (Vellosillo et al., 2007). As with 9-HOT and 9-KOT, these 13-LOX and α-DOX derivatives fail to induce a root-waving phenotype in the *bri1* mutant (BR signaling defective; Supplemental Fig. S3), which indicates that BR signaling mediates their activity. Like with 9-LOX derivatives, 13-LOX and α-DOX products could be generated during pathogen infection, contributing to activate cell wall-based defense. The production of oxylipins with cell wall-modifying activity from distinct biosynthetic pathways could help to compensate the lack of 9-LOX derivatives in the *lox1lox5* mutants.

Cell wall modification, including callose deposit formation, is an important plant response that limits pathogen infection (Vorwerk et al., 2004; Luna et al., 2011). High levels of callose production in *bes1-D* mutants (constitutively active BR pathway) correlate with enhanced resistance to *Pseudomonas* spp. infection, whereas *noxy2-2* mutants, with low levels of callose deposits, are susceptible to this bacterium (Vellosillo et al., 2013). Nonetheless, resistance to pathogen infection does not always correlate with callose deposition levels (Nishimura et al., 2003). This is the case for *lox1lox5* mutants, in which lack of 9-LOX activity enhances susceptibility to *Pseudomonas* spp. inoculation (Hwang and Hwang, 2010; López et al., 2011), even though callose production in bacterially infected leaves did not vary with respect to wild-type plants. Although callose production in *bzr1-1D* mutant leaves was similar, in these plants, constitutive activation of BR signaling increased resistance to *Pseudomonas* spp. infection (Fig. 6). Based on callose deposit formation, bacterial growth, and symptom development, the defense potential to *Pseudomonas* spp. infection is lower in *bzr1-1D* than in *bes1-D* mutants, which might reflect the reduced BR activation in *bzr1-1D* plants.

Involvement of the 9-LOX and BR signaling pathways in the induction of cell wall-based defense is

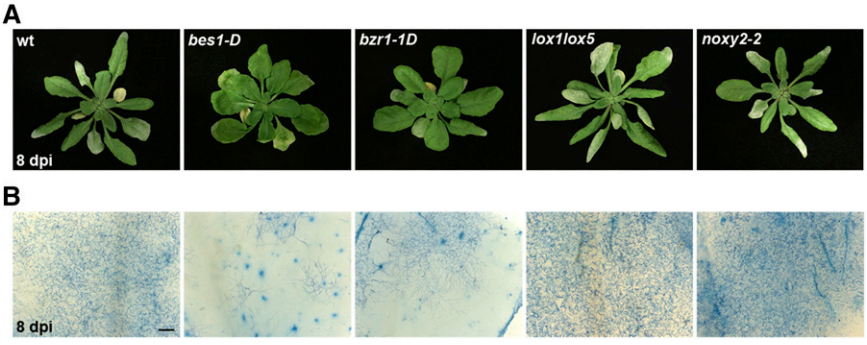

Figure 7. Responses of wild-type (wt), *bes1-D*, *brz1-1D*, *lox1lox5*, and *noxy2-2* plants to infection with *G. cichoracearum*. A, Phenotypes of plants at 8 d postinoculation. B, Coomassie Brilliant Blue staining of infected leaves. Representative examples of symptoms are shown from three independent experiments. Bar = 500 μm.

further supported by results with *G. cichoracearum*, an obligate biotrophic fungus that feeds from living cells after penetrating the epidermal cell wall (Micali et al., 2008). In these studies, constitutive activation of BR signaling in *bes1-D* and *bzr1-1D* mutants impaired fungal infection, suggesting cell wall reinforcement, whereas enhanced susceptibility in *lox1lox5* and *noxy2-2* mutants is consistent with a weakened cell wall. Cell wall lignification at the site of attempted penetration of biotrophic fungi is considered a first line of defense (Bhuiyan et al., 2009) and could be linked to resistance/susceptibility responses to *G. cichoracearum* in the mutants examined here. In line with this discussion, we note that treatment with the cellulose synthesis inhibitor isoxaben induces ectopic lignin accumulation in wild-type plants but not in *det2-1* and *noxy2-2* mutants (Supplemental Fig. S4). Reversion of this defect in *det2-1* but not in *noxy2-2* plants by BL application (Supplemental Fig. S4) confirms the participation of the 9-LOX and BR pathways in activating lignin deposition and, thus, cell wall repair, a reaction that could influence *G. cichoracearum* penetration.

9-HOT and 9-KOT induce ROS or act as reactive electrophile species to trigger transcriptional reprogramming or to modify macromolecules covalently (Vellosillo et al., 2007; Mueller et al., 2008; López et al., 2011; Vicente et al., 2012; Farmer and Mueller, 2013; Montillet et al., 2013). Plant responses to these oxylipins are under mitochondrial retrograde control, as 9-HOT causes mitochondrial aggregation and loss of mitochondrial membrane potential and *NOXY2* (and the 9-LOX signaling *NOXY* genes *DYNAMIN-RELATED PROTEIN3A/NOXY15* and *FRIENDLY MITOCHONDRIA/NOXY38*) encodes a mitochondrial protein (Vellosillo et al., 2013). Our results show the interaction between 9-LOX and BR pathways and locate *NOXY2* (Fig. 4) and likely *NOXY15* and *NOXY38* (Supplemental Fig. S5) upstream of BRs. Mitochondria are a major source of ROS and act as signaling organelles that coordinate plant growth and defense (Huang, et al., 2013; Nie et al., 2015). Mitochondria dysfunction interferes with 9-LOX and BR signaling (Bekh-Ochir et al., 2013; Vellosillo et al., 2013) and might unbalance ROS production, a key process in the control of plant development and plant defense. Recent studies indicate BR pathway involvement in plant immunity and its role in balancing defense versus growth (Belkhadir et al., 2014; Fan et al., 2014). Our results show the sequential participation of the 9-LOX and BR pathways in triggering cell wall-based plant defense; in response to pathogen inoculation, oxylipins might function as ROS signals to activate the BR pathway and contribute to cell wall reinforcement and plant defense.

MATERIALS AND METHODS

Plants and Growth Conditions

The mutants *noxy2-2* (oxylipin insensitive), *lox1lox5* (9-LOX deficient), *bri1-1* (BR insensitive), *det2-1* (BR deficient), and *bes1-D* and *bzr1-1D* (constitutively active BR signaling) and the transgenic lines BKI1:YFP, BZR1:CFP, and BZR2/BES1:GFP were derived from Arabidopsis (*Arabidopsis thaliana*) ecotype Columbia-0 plants. The transgenic line *DRWF4:GUS* was derived from Arabidopsis ecotype Wassilewskija-2 plants. For in vitro analyses, sterilized seeds were vernalized (3 d at 4°C) and allowed to grow on plates containing MS medium, pH 6, with 1.5% (w/v) Suc and 1.5% or 0.8% (w/v) agar (Bacto Agar; Becton-Dickinson) for vertical or horizontal plates, respectively; growth conditions were 14 h of light and 10 h of dark, 22°C, and 250 μE m^{-2} s^{-1} fluorescent illumination. For phenotype analysis, seeds were transferred 3 d postgermination to plates containing 9-HOT (25 μM), 9-KOT (25 μM), BL (10 nM), or BZ (1 μM). Oxylipin stocks were prepared as described (López et al., 2011) and then diluted in water to a final concentration. To evaluate hypocotyl length, seeds were germinated on MS vertical plates and grown in conditions of high-light (250 μE m^{-2} s^{-1} in 14 h of light and 10 h of dark) or low-light (50 μE m^{-2} s^{-1} in 8 h of light and 16 h of dark) fluorescent illumination. Plates were placed vertically and scanned; hypocotyl length was measured using the ImageJ program (http://imagej.nih.gov/ij/). One-way ANOVA and Games-Howell tests were used to determine the significance of differences between data sets from seedlings grown in the two light conditions examined. Unless stated otherwise, phenotypes were analyzed 7 d after seed germination in approximately 15 seedlings in at least three independent experiments. For in planta analyses, seeds were sown on soil, vernalized (3 d at 4°C), and grown in chambers (22°C, 70% relative humidity, with a 14-h-light/10-h-dark photoperiod at 250 μE m^{-2} s^{-1} fluorescent illumination). Plants were treated and examined between 3 and 4 weeks after seed germination.

RNA Isolation and Analysis of Gene Expression

To examine gene expression, seeds were germinated on horizontal or vertical plates; at 12 d postgermination, they were treated with 9-KOT (25 μM) or BL (1 μM). Plant tissues for RNA extraction were collected at various intervals, frozen in liquid nitrogen, and stored at −80°C. Total RNA was isolated according to Logemann et al. (1987). RNA was treated with DNase TURBO DNA-free (Ambion) to remove contaminating DNA; a 1-μg RNA sample was used in each one-step RT-PCR. For RT-PCR, we used a GeneAmp PCR System 9700 thermal cycler (Applied Biosystems) with the Transcriptor First Strand complementary DNA synthesis kit (Roche Applied Science). Gene expression was quantified by quantitative RT-PCR analyses using the 7500 Real-Time PCR system (Applied Biosystems) and FastStart Universal SYBR Green Master (Roche). Accession numbers for the genes analyzed are as follows: *ABC* (At1g15520), *FOX* (At1g26380), *EXP8* (At2g40610), and *RPL3A* (At1g43170; used as an internal control). Primers for these analyses and the lengths of amplification products are described in Supplemental Table S1.

Protein Extraction and Western Blot

Six-day-old seedlings of *BZR1-CFP* or *BZR2/BES1-GFP* transgenic plants were transferred to liquid MS medium and treated with BL (50 nM) alone or combined with 25 μM 9-HOT or 9-KOT. For protein extraction, seedlings were collected at various intervals, frozen in liquid nitrogen, and stored at −80°C. Protein extracts were prepared by grinding seedlings to a fine powder in liquid nitrogen and extracted with 50 mM Tris-HCl, pH 7.5, 150 mM NaCl, 0.1% (w/v) Nonidet P-40, 1 mM phenylmethylsulfonyl fluoride, and 1× complete protease inhibitor cocktail (Roche). Supernatants were centrifuged (3,000*g*, 10 min, and 4°C), separated by 7.5% SDS-PAGE, and transferred to nitrocellulose membranes by electroblotting. Immunoblot assays were performed as described (Sanz et al., 1998) using anti-GFP antibodies (Clontech) and 0.1% (w/v) Ponceau Red staining as a control for protein loading.

Histological Analyses

For callose detection, roots were stained with an Aniline Blue fluorochrome solution (0.1 mg mL^{-1}; SiroBiosupplies; 30 min, in the dark). Samples were washed, mounted in 50% glycerol on glass microscope slides, and examined with a Leica DMR fluorescence microscope. Callose in leaves was stained as for roots. Three leaves each from 4-week-old plants were inoculated with a suspension of 10^6 cfu mL^{-1} *Pseudomonas syringae* pv *tomato* DC3000 (grown for 24 h on plates containing King's medium) and excised from plants 24 h after inoculation. Controls were inoculated with $MgCl_2$ (10 mM). Leaves were washed in an ethanol solution before staining (30 min in the dark). Samples were washed, mounted on slides, and examined with a Leica DMI 6000B epifluorescence microscope. The size and number of callose deposits were quantified with ImageJ. For each genotype, 10 or more plants were examined in three independent experiments. Data were analyzed statistically by Student's *t* test (***, $P < 0.001$; **, $0.001 < P < 0.01$;

and *, $0.01 < P < 0.05$). YFP fluorescent images were generated on a Leica TCS-SP5 confocal microscope with LAS AF version 2.6.0 software using a 63×/1.2 numerical aperture water-immersion objective and sequential scanning with argon at 488 nm. GUS activity in *DRWF4:GUS* transgenic plants was examined as described (Vellosillo et al., 2007).

In Vivo Analyses of Growth and Bacterial Symptoms

Pst DC3000 inoculations were performed in greenhouse conditions by injecting a suspension (10^5 cfu mL^{-1}) into the leaf apoplasts. Bacterial suspensions were prepared as above. Discs from infected leaves were excised at 3 d postinoculation, pooled in triplicate, homogenized, and used to count bacterial growth on petri plates. The results show means ± SE of values for three independent experiments. Data were analyzed statistically by Student's *t* test (***, $P < 0.001$; **, $0.001 < P < 0.01$; and *, $0.01 < P < 0.05$) using GraphPad PRIMS version 4 software. For symptom tests, plants were examined at 3 d after bacterial infiltration (10^6 cfu mL^{-1}). Phenotypic symptoms were rated on a three-point scale designated as I, II, and III according to their severity, and the percentages of leaves showing each type of symptom were quantified. The results show means ± SE of values for three independent experiments.

In Vivo Analyses of *Golovinomyces cichoracearum* Infection

Three-week-old plants were inoculated with *G. cichoracearum* using a settling tower as described (Vogel and Somerville, 2000). For the visualization of fungal structures, plants were harvested at the indicated times, destained, and stored in 3:1 (v/v) ethanol:glacial acetic acid. Fungal structures were stained with Coomassie Brilliant Blue as described (Göllner et al., 2008).

Sequence data from this article can be found in the GenBank/EMBL data libraries under accession numbers *ABC* (At1g15520), *FOX* (At1g26380), *EXP8* (At2g40610), and *RPL3A* (At1g43170).

Supplemental Data

The following supplemental materials are available.

Supplemental Figure S1. Activation of BR signaling by 9-HOT and 9-KOT.

Supplemental Figure S2. Correspondence between 9-KOT-induced and BR-regulated genes.

Supplemental Figure S3. Phenotypic response of *bri1-1* mutant seedlings to oxylipins.

Supplemental Figure S4. Lignin deposition in wild type, *det2-1*, and *noxy2-2* after isoxaben treatment.

Supplemental Figure S5. Phenotypic response of *noxy15* and *noxy38* mutants to BR.

Supplemental Table S1. Set of primers used to examine gene expression.

ACKNOWLEDGMENTS

We thank Shauna Somerville and Heidi Szemenyei for advice with fungal infection; Joanne Chory and Zhi-Yong Wang for BKI1:CYP, BZR1:CFP, and BZR2/BES1:GFP transgenic lines and *bes1-D* and *bzr1-1D* mutants; Sunghwa Choe for the *DWF4:GUS* transgenic line; Heidi Szemenyei for help with fungal infection; Sylvia Gutiérrez and Laura Cuyás for help with confocal microscopy; Raquel Piqueras for help with in vitro plant growth; Inés Poveda for photography; Gunvor Hamberg for assistance during the preparation of the oxylipins; and Catherine Mark for editorial assistance.

Received July 7, 2015; accepted September 28, 2015; published September 28, 2015.

LITERATURE CITED

Andreou A, Brodhun F, Feussner I (2009) Biosynthesis of oxylipins in non-mammals. Prog Lipid Res **48:** 148–170

Bannenberg G, Martínez M, Rodríguez MJ, López MA, Ponce de León I, Hamberg M, Castresana C (2009) Functional analysis of α-DOX2, an active α-dioxygenase critical for normal development in tomato plants. Plant Physiol **151:** 1421–1432

Bekh-Ochir D, Shimada S, Yamagami A, Kanda S, Ogawa K, Nakazawa M, Matsui M, Sakuta M, Osada H, Asami T, et al (2013) A novel mitochondrial DnaJ/Hsp40 family protein BIL2 promotes plant growth and resistance against environmental stress in brassinosteroid signaling. Planta **237:** 1509–1525

Belkhadir Y, Yang L, Hetzel J, Dangl JL, Chory J (2014) The growth-defense pivot: crisis management in plants mediated by LRR-RK surface receptors. Trends Biochem Sci **39:** 447–456

Bhuiyan NH, Selvaraj G, Wei Y, King J (2009) Gene expression profiling and silencing reveal that monolignol biosynthesis plays a critical role in penetration defence in wheat against powdery mildew invasion. J Exp Bot **60:** 509–521

Blée E (2002) Impact of phyto-oxylipins in plant defense. Trends Plant Sci **7:** 315–322

Boller T, Felix G (2009) A renaissance of elicitors: perception of microbe-associated molecular patterns and danger signals by pattern-recognition receptors. Annu Rev Plant Biol **60:** 379–406

Browse J (2009) Jasmonate passes muster: a receptor and targets for the defense hormone. Annu Rev Plant Biol **60:** 183–205

Chung Y, Maharjan PM, Lee O, Fujioka S, Jang S, Kim B, Takatsuto S, Tsujimoto M, Kim H, Cho S, et al (2011) Auxin stimulates DWARF4 expression and brassinosteroid biosynthesis in Arabidopsis. Plant J **66:** 564–578

Dangl JL, Horvath DM, Staskawicz BJ (2013) Pivoting the plant immune system from dissection to deployment. Science **341:** 746–751

Durand T, Bultel-Poncé V, Guy A, Berger S, Mueller MJ, Galano JM (2009) New bioactive oxylipins formed by non-enzymatic free-radical-catalyzed pathways: the phytoprostanes. Lipids **44:** 875–888

Fan M, Bai MY, Kim JG, Wang T, Oh E, Chen L, Park CH, Son SH, Kim SK, Mudgett MB, et al (2014) The bHLH transcription factor HBI1 mediates the trade-off between growth and pathogen-associated molecular pattern-triggered immunity in *Arabidopsis*. Plant Cell **26:** 828–841

Farmer EE, Mueller MJ (2013) ROS-mediated lipid peroxidation and RES-activated signaling. Annu Rev Plant Biol **64:** 429–450

Ferrari S, Savatin DV, Sicilia F, Gramegna G, Cervone F, Lorenzo GD (2013) Oligogalacturonides: plant damage-associated molecular patterns and regulators of growth and development. Front Plant Sci **4:** 49

Fonseca S, Chini A, Hamberg M, Adie B, Porzel A, Kramell R, Miersch O, Wasternack C, Solano R (2009) (+)-7-iso-Jasmonoyl-L-isoleucine is the endogenous bioactive jasmonate. Nat Chem Biol **5:** 344–350

Friedrichsen DM, Joazeiro CA, Li J, Hunter T, Chory J (2000) Brassinosteroid-insensitive-1 is a ubiquitously expressed leucine-rich repeat receptor serine/threonine kinase. Plant Physiol **123:** 1247–1256

Fujioka S, Li J, Choi YH, Seto H, Takatsuto S, Noguchi T, Watanabe T, Kuriyama H, Yokota T, Chory J, et al (1997) The *Arabidopsis deetiolated2* mutant is blocked early in brassinosteroid biosynthesis. Plant Cell **9:** 1951–1962

Göllner K, Schweizer P, Bai Y, Panstruga R (2008) Natural genetic resources of Arabidopsis thaliana reveal a high prevalence and unexpected phenotypic plasticity of RPW8-mediated powdery mildew resistance. New Phytol **177:** 725–742

Hamann T, Bennett M, Mansfield J, Somerville C (2009) Identification of cell-wall stress as a hexose-dependent and osmosensitive regulator of plant responses. Plant J **57:** 1015–1026

Hamberg M, Ponce de León I, Sanz A, Castresana C (2002) Fatty acid alpha-dioxygenases. Prostaglandins Other Lipid Mediat **68-69:** 363–374

Hamberg M, Sanz A, Rodriguez MJ, Calvo AP, Castresana C (2003) Activation of the fatty acid alpha-dioxygenase pathway during bacterial infection of tobacco leaves: formation of oxylipins protecting against cell death. J Biol Chem **278:** 51796–51805

Huang Y, Chen X, Liu Y, Roth C, Copeland C, McFarlane HE, Huang S, Lipka V, Wiermer M, Li X (2013) Mitochondrial AtPAM16 is required for plant survival and the negative regulation of plant immunity. Nat Commun **4:** 2558

Hwang IS, Hwang BK (2010) The pepper 9-lipoxygenase gene *CaLOX1* functions in defense and cell death responses to microbial pathogens. Plant Physiol **152:** 948–967

Jung HW, Tschaplinski TJ, Wang L, Glazebrook J, Greenberg JT (2009) Priming in systemic plant immunity. Science **324:** 89–91

Kachroo A, Kachroo P (2009) Fatty acid-derived signals in plant defense. Annu Rev Phytopathol **47:** 153–176

Lanza M, Garcia-Ponce B, Castrillo G, Catarecha P, Sauer M, Rodriguez-Serrano M, Páez-García A, Sánchez-Bermejo E, Mohan TC, Leo del Puerto

Y, et al (2012) Role of actin cytoskeleton in brassinosteroid signaling and in its integration with the auxin response in plants. Dev Cell **22:** 1275–1285

Logemann J, Schell J, Willmitzer L (1987) Improved method for the isolation of RNA from plant tissues. Anal Biochem **163:** 16–20

López MA, Bannenberg G, Castresana C (2008) Controlling hormone signaling is a plant and pathogen challenge for growth and survival. Curr Opin Plant Biol **11:** 420–427

López MA, Vicente J, Kulasekaran S, Vellosillo T, Martínez M, Irigoyen ML, Cascón T, Bannenberg G, Hamberg M, Castresana C (2011) Antagonistic role of 9-lipoxygenase-derived oxylipins and ethylene in the control of oxidative stress, lipid peroxidation and plant defence. Plant J **67:** 447–458

Luna E, Pastor V, Robert J, Flors V, Mauch-Mani B, Ton J (2011) Callose deposition: a multifaceted plant defense response. Mol Plant Microbe Interact **24:** 183–193

Macho AP, Zipfel C (2014) Plant PRRs and the activation of innate immune signaling. Mol Cell **54:** 263–272

Manfield IW, Orfila C, McCartney L, Harholt J, Bernal AJ, Scheller HV, Gilmartin PM, Mikkelsen JD, Knox JP, Willats WG (2004) Novel cell wall architecture of isoxaben-habituated Arabidopsis suspension-cultured cells: global transcript profiling and cellular analysis. Plant J **40:** 260–275

Micali C, Göllner K, Humphry M, Consonni C, Panstruga R (2008) The powdery mildew disease of Arabidopsis: a paradigm for the interaction between plants and biotrophic fungi. The Arabidopsis Book **6:** e0115, doi/10.1199/tab.0115

Montillet JL, Leonhardt N, Mondy S, Tranchimand S, Rumeau D, Boudsocq M, Garcia AV, Douki T, Bigeard J, Laurière C, et al (2013) An abscisic acid-independent oxylipin pathway controls stomatal closure and immune defense in Arabidopsis. PLoS Biol **11:** e1001513

Mueller S, Hilbert B, Dueckershoff K, Roitsch T, Krischke M, Mueller MJ, Berger S (2008) General detoxification and stress responses are mediated by oxidized lipids through TGA transcription factors in *Arabidopsis*. Plant Cell **20:** 768–785

Nalam VJ, Keeretaweep J, Sarowar S, Shah J (2012) Root-derived oxylipins promote green peach aphid performance on *Arabidopsis* foliage. Plant Cell **24:** 1643–1653

Nie S, Yue H, Zhou J, Xing D (2015) Mitochondrial-derived reactive oxygen species play a vital role in the salicylic acid signaling pathway in Arabidopsis thaliana. PLoS One **10:** e0119853

Nishimura MT, Stein M, Hou BH, Vogel JP, Edwards H, Somerville SC (2003) Loss of a callose synthase results in salicylic acid-dependent disease resistance. Science **301:** 969–972

Obregón P, Martín R, Sanz A, Castresana C (2001) Activation of defence-related genes during senescence: a correlation between gene expression and cellular damage. Plant Mol Biol **46:** 67–77

Santino A, Taurino M, De Domenico S, Bonsegna S, Poltronieri P, Pastor V, Flors V (2013) Jasmonate signaling in plant development and defense response to multiple (a)biotic stresses. Plant Cell Rep **32:** 1085–1098

Sanz A, Moreno JI, Castresana C (1998) PIOX, a new pathogen-induced oxygenase with homology to animal cyclooxygenase. Plant Cell **10:** 1523–1537

Shimada TL, Takano Y, Shimada T, Fujiwara M, Fukao Y, Mori M, Okazaki Y, Saito K, Sasaki R, Aoki K, et al (2014) Leaf oil body functions as a subcellular factory for the production of a phytoalexin in Arabidopsis. Plant Physiol **164:** 105–118

Sun Y, Fan XY, Cao DM, Tang W, He K, Zhu JY, He JX, Bai MY, Zhu S, Oh E, et al (2010) Integration of brassinosteroid signal transduction with the transcription network for plant growth regulation in Arabidopsis. Dev Cell **19:** 765–777

Vellosillo T, Aguilera V, Marcos R, Bartsch M, Vicente J, Cascón T, Hamberg M, Castresana C (2013) Defense activated by 9-lipoxygenase-derived oxylipins requires specific mitochondrial proteins. Plant Physiol **161:** 617–627

Vellosillo T, Martínez M, López MA, Vicente J, Cascón T, Dolan L, Hamberg M, Castresana C (2007) Oxylipins produced by the 9-lipoxygenase pathway in *Arabidopsis* regulate lateral root development and defense responses through a specific signaling cascade. Plant Cell **19:** 831–846

Vicente J, Cascón T, Vicedo B, García-Agustín P, Hamberg M, Castresana C (2012) Role of 9-lipoxygenase and α-dioxygenase oxylipin pathways as modulators of local and systemic defense. Mol Plant **5:** 914–928

Vogel J, Somerville S (2000) Isolation and characterization of powdery mildew-resistant Arabidopsis mutants. Proc Natl Acad Sci USA **97:** 1897–1902

Vorwerk S, Somerville S, Somerville C (2004) The role of plant cell wall polysaccharide composition in disease resistance. Trends Plant Sci **9:** 203–209

Wang C, El-Shetehy M, Shine MB, Yu K, Navarre D, Wendehenne D, Kachroo A, Kachroo P (2014) Free radicals mediate systemic acquired resistance. Cell Reports **7:** 348–355

Wang X, Chory J (2006) Brassinosteroids regulate dissociation of BKI1, a negative regulator of BRI1 signaling, from the plasma membrane. Science **313:** 1118–1122

Wang ZY, Nakano T, Gendron J, He J, Chen M, Vafeados D, Yang Y, Fujioka S, Yoshida S, Asami T, et al (2002) Nuclear-localized BZR1 mediates brassinosteroid-induced growth and feedback suppression of brassinosteroid biosynthesis. Dev Cell **2:** 505–513

Wasternack C, Hause B (2013) Jasmonates: biosynthesis, perception, signal transduction and action in plant stress response, growth and development. An update to the 2007 review in Annals of Botany. Ann Bot (Lond) **111:** 1021–1058

Weigel D, Glazebrook J (2008) Genetic analysis of Arabidopsis mutants. CSH Protoc **2008:** pdb.top35

Wittek F, Hoffmann T, Kanawati B, Bichlmeier M, Knappe C, Wenig M, Schmitt-Kopplin P, Parker JE, Schwab W, Vlot AC (2014) Arabidopsis ENHANCED DISEASE SUSCEPTIBILITY1 promotes systemic acquired resistance via azelaic acid and its precursor 9-oxo nonanoic acid. J Exp Bot **65:** 5919–5931

Wolf S, Höfte H (2014) Growth control: a saga of cell walls, ROS, and peptide receptors. Plant Cell **26:** 1848–1856

Wolf S, Mravec J, Greiner S, Mouille G, Höfte H (2012) Plant cell wall homeostasis is mediated by brassinosteroid feedback signaling. Curr Biol **22:** 1732–1737

Wrzaczek M, Brosché M, Kangasjärvi J (2013) ROS signaling loops: production, perception, regulation. Curr Opin Plant Biol **16:** 575–582

Wu J, Baldwin IT (2010) New insights into plant responses to the attack from insect herbivores. Annu Rev Genet **44:** 1–24

Yin Y, Wang ZY, Mora-Garcia S, Li J, Yoshida S, Asami T, Chory J (2002) BES1 accumulates in the nucleus in response to brassinosteroids to regulate gene expression and promote stem elongation. Cell **109:** 181–191

Zhu JY, Sae-Seaw J, Wang ZY (2013) Brassinosteroid signalling. Development **140:** 1615–1620

Zoeller M, Stingl N, Krischke M, Fekete A, Waller F, Berger S, Mueller MJ (2012) Lipid profiling of the Arabidopsis hypersensitive response reveals specific lipid peroxidation and fragmentation processes: biogenesis of pimelic and azelaic acid. Plant Physiol **160:** 365–378